We thank Referee 1 for the valuable comments and suggestions. Our responses to each point follow. (Please note that we plan to convert our Appendix to a Supplement.)

1. In page 10820 line 12: you mention that some authors highlighted that human influence as a function of human population density are poorly explained and you aknowledge the work of Prentice et al., 2010. However, Prentice et al., did not show that with a data driven analysis. In my opinion work like: [Knorr, W., Kaminski, T., Arneth, a., & Weber, U. (2014). Impact of human population density on fire frequency at the global scale. Biogeosciences, 11, 1085-1102] and [Bistinas, I., Oom, D., Sa, A. C. L., Harrison, S. P., Prentice, I. C., & Pereira, J. M. C. (2013). Relationships between human population density and burned area at continental and global scales. PLoS ONE, 8] should be acknowledged. The first study shows a non-linear model estimating the effect of population density on burnt area at global scale. The second study (and very relevant to the current paper) highlights that the effect of population density on fires in fact a function of land use changes and considers the agriculture being two of them.

Bistinas et al. (2013) is indeed extremely relevant and we thank the referee for bringing it to our attention. We will replace the citation of Prentice et al. (2011) with these two articles.

2. Page 10824, line 16: Why not using GFED4 for that study? The native resolution of GFED4 is 0.25°, but GFED3 is at 0.5°. However, from the description you make, it looks like it's a typing error and that you indeed used the 4th version. If not, I would totally recommend to update your calculations.

While GFED3 is distributed at 0.5° resolution, the underlying algorithm actually produces raw data at a much finer resolution. In producing GFED3s, Randerson et al. (2012) appear to have decided that the benefit of distributing the data at 0.25° outweighs any additional infrastructure costs (e.g., server space, bandwidth). We chose GFED3s rather than GFED4 because GFED3s focused specifically on capturing burned area and emissions from small fires, which we hypothesized would be especially important for agricultural burning.

3. Page 10827, line 1: You write that "Fuel load should be higher on average for non- agricultural lands than for pasture because pastures do not have trees in densities comparable to more carbon-rich forest ecosystems." That is not entirely correct as in pastures, the low vegetation has high postfire regeneration and can be prone to more than one fire events. Especially in savanna biomes.

We agree that the high frequency of fire in savanna could lead to higher average annual emissions there than in a higher-biomass but less-burned ecosystem. However, this difference is in total fuel *consumption*, not fuel *load* or fuel consumption/emissions *per area burned*. Fuel load is simply the amount of fuel available to burn at any given time. Fuel consumption in a savanna would indeed be higher if it were to burn twice, but its emissions per area burned are a function of fuel load only. van der Werf et al. (2010), in the paper analyzing

GFED3 fire emissions estimates, agree:

> Fuel consumption (reported here as gC per m^2 of area burned) broadly followed biome distributions with low biomass density biomes such as grasslands and savannas burning less fuel than high biomass density types such as forests.

We will thus add a citation of van der Werf et al. (2010) to the end of the sentence you quoted to support this idea.

4. Page 10827, line 13: How well they reproduce the patterns? Please provide some metrics at this point already.

We will add a figure to the Supplement illustrating the results with regard to total fire in GFED regions, in the same style as Figure 8a. We will also discuss the statistics (linear regression slope, intercept, and Pearson's r) at this point to illustrate how close to the 1:1 line the points lie.

5. Figure 4: besides mean annual burnt area, the most intuitive way to show your results here would be seasonal means for December-January-February and so on (MAM, JJA, SON).

We will add maps of seasonal means to the Supplement.

We thank Referee 2 for the valuable comments and suggestions. Our responses to each point follow. (Please note that we plan to convert our Appendix to a Supplement.)

Please add numbering to the equations.
We will do so.

In equation 2, (line 4 on page 10822) you optimize $\widehat{F_{k,i}}$ where k stands for c, p or o. However, you minimize the sum of squared errors for each analysis region (or group of grid cells), let's say r, and not for each grid cell i. It may thus be better to use something like where r is the analysis region (or cluster of grid cells), and k may be c, p or o.

Thank you for finding that error; we apologize for the confusion. The symbols referred to in equation 2 were not supposed to have had the i subscript, so we will correct that. We will likely not add an r subscript, instead just leaving off the i subscript and using the "hat," which together we feel sufficiently distinguish the region-month Fs from those referring to individual grid cells.

To continue, in your first equation on page 10821 $\widehat{F_{k,i}}$ stands for the "fraction of that land-use type that burned in that grid cell". However, when optimizing in the next equation (first equation on p. 10822) $\widehat{F_{k,i}}$ values represent a different thing: the slopes of multiple linear regression between the spatial distribution of BA and the three land use types. This means that $\widehat{F_{k,i}}$ cannot be interpreted exactly the same as $F_{k,i}$ and is not "the fraction of land-use type that burns across the region". It would help the reader if you would redefine and clearly state what $\widehat{F_{k,i}}$ stands for, and then if you want to explain it in a less technical way you could state "this is related to the fraction of land-use type that burns across the region".

The $\widehat{F_k}$ values are indeed analogous to the unknown slopes that are solved for in multiple linear regression. They tell us that, for example, in a region with $\widehat{F_p} = 1$, a grid cell with 110 ha of pasture (and equal amounts of cropland and non-agricultural land) will have one more hectare of burned area than a grid cell with 100 ha of pasture. However, this analogy does not preclude interpretation of the values as best-guess estimates of region-wide fractional burning of each land cover.

As written in the paper: "The values of each $F_{k,i}$ are unknown, but a best-guess $\widehat{F_k}$ can be estimated across a group of N grid cells" (p. 10822, lines 23). That is, because we don't know the value of each $F_{k,i}$, we instead calculate $\widehat{F_k}$, which is one number that we plug in as a best-guess estimate for each $F_{k,i}$ (i.e., into Eqn. 1: p. 10821, line 25).

We can put this conceptualization into equation form. Consider the total burned area across a region (B_r) as the sum of the burned areas in each grid cell i:

$$B_r = B_1 + ... + B_i + ... + B_N$$

$$B_i = F_{c,i}A_{c,i} + F_{p,i}A_{p,i} + F_{o,i}A_{o,i}$$

$$B_r = \sum_{i=1}^{N} (F_{c,i}A_{c,i} + F_{p,i}A_{p,i} + F_{o,i}A_{o,i})$$

This is essentially where we are with Equation 2 in the manuscript—we don't know every $F_{k,i}$, so we need to find best-guess estimates:

$$B_r \approx \sum_{i=1}^{N} (\widehat{F_c}A_{c,i} + \widehat{F_p}A_{p,i} + \widehat{F_o}A_{o,i})$$

In the manuscript, we then describe the method by which we find these best-guess estimates (using an algorithm, unsurprisingly, that is commonly used by statistical software to fit multiple linear regressions!). But we can go a bit further here:

$$B_r \approx \widehat{F_c} \sum_{i=1}^{N} A_{c,i} + \widehat{F_p} \sum_{i=1}^{N} A_{p,i} + \widehat{F_o} \sum_{i=1}^{N} A_{o,i}$$

$$B_r \approx \widehat{F_c}A_{c,r} + \widehat{F_p}A_{p,r} + \widehat{F_o}A_{o,r}$$

Thus, the $\widehat{F_k}$ values do indeed represent best guesses of fractional burning of each land cover type across the region.

The second definition (P10823 L12) "the net effect of land use k on fire in the region, expressed as a fraction of the area of land use k in the region" is confusing.

We will edit/add text to clarify this idea.

The negative slopes are interesting and I agree that they may well represent a real aspect of the system. But with this definition you undermine your more realistic interpretation that a certain land use may affect fire activity in different land use classes in the vicinity (often within the same 0.25 grid cell).

We will reiterate, in the same paragraph as the text referenced in the above comment, that the negative effect of some some land use is indeed felt on other land uses.

The Methods of GFED are explained by van der Werf et al., 2010, and adjusted by Randerson et al., 2012.

We will add a citation of van der Werf et al. (2010) in addition to the reference to Giglio et al. (2010) when discussing GFED3 and GFED3s.

Figures 2 and 3. It would be easier for the reader if you would just present the annual burned area and carbon emissions split up by the different land use types (k) here.

In our estimation, the graphical presentation in Figures 2 and 3 makes it easy for the reader to extract important information at a glance. For example, one can get a sense of interannual variability more easily than if given a mean ± s.d. For another example, one can easily grasp that although at a global scale

(and for many regions) there is almost as much burned area associated with pasture as with non-agricultural lands, pasture fires are associated with much lower emissions levels. Thus, we feel it is important to keep the time series plots. However, for readers interested in the numbers behind Figure 3, we will add a table to the Supplement.

Then you can remove the "cropland and crop+ categories" which are confusing and just use one "total".

It is important to distinguish between what the remote sensing algorithm classifies as "cropland" and "cropland-natural mosaic" because, when fire occurs on mosaic, we cannot be sure whether it is the cropland that is actually burning. We thus might expect the actual amount of burned cropland to be more than that on "cropland" but less than that on combined "cropland plus cropland-natural mosaic." The latter is what we refer to as "Crop+" in the figures. To reduce confusion, we will add text explaining "Crop+" to Figure 3.

It is not clear what applying the "model" adds to the results presented in these two figures opposed to a simple estimate of burned area per land use type "crop, pasture, natural, total".

The total estimated ("model") burning is included in these figures for comparison with the total observed burning, as a first-order check of the results. If the estimated and observed total burning differed greatly, then the reader would know to be extra cautious in interpreting the partitioned fire activity.

The authors provide little insights in the model performance and background data-sets. How much of the spatial variation in burned area can be explained by the distribution of the three land use classes for each analysis region (e.g., r-squared)?

We will add, to Section 4.3, some discussion of overall R-squared as it relates to the amount of variation in burned area that can be explained by land cover distributions.

What are the actual $\widehat{F_{k,i}}$ values per analysis region? And what does the land use distribution look like? It would be interesting to see some of these figures either in the main body of text or in the Annex material.

We will add a table of $\widehat{F_k}$ values for every month and region to the Supplement, along with maps of mean land cover distributions.

If you think the paper is becoming too long you could merge figures 2 and 3, or remove all the current annex figures and make your point about the current interpretation of negative $\widehat{F_{k,i}}$ a little stronger by citing more literature.

We will likely not merge Figures 2 and 3, but will add more literature supporting the idea of negative $\widehat{F_k}$ values to the paragraph where that idea is introduced (p. 10822).

Fig. 4, this is an interesting figure. You state that "Numbers can be in-

terpreted as ..", but for the reader it would be easier if you first state what the numbers actually are, something like "the maps show times the area of k". Then in the next phrase you can say, "this can be interpreted as..". Many people have knowledge about these type of models, providing such information makes it easier for them to interpret your results.

We will add some text to this effect to the captions of Figures 4 and A3.

Figures 5 and 8, it seems that many of the regions are resolved as "mean" values, and that the different land use types provide only limited information on the spatial distribution of annual burned area within the analysis regions. This may be a consequence of: (1) Burned area in many analysis regions is dominated by a single land use. (2) In many cases little of the spatial distribution of BA can be explained by land use. Both will make the values converge to the mean. This should be more clearly discussed.

We will add some discussion of this phenomenon to Section 4.3.

Figure 7a, please explain the meaning of the three colors in the caption of the figure. Figure 7b, It may look nicer if you would delete the white space on the x-axis before "August".

We will make these changes.

Figure 8b. This figure is a little counter intuitive now. First you say "(b) each grid cell", but then the fit and the equations are presented for binned-mean values. First, depending on your bin-size the slope and r-squared will vary, which makes the results subjective. Second, you have already presented the "binned" results in Fig. 8a (using analysis regions for bins). It would be interesting to read here how much of the spatial variation in burned area is actually captured at the grid cell level by your model.

We will add text to the captions of Figures 8 and A7 clarifying that bins are being used. We do believe, however, that both subfigures A and B are necessary. 8a/A7a illustrate the point that the algorithm is very good at estimating total burned area across a region, while 8b/A7b show that much less of the variation at the level of individual grid cells is captured. We will add more discussion of the results presented in these figures, including R-squared of gridcell-level variation, to Section 4.3.

For the reader it may be easier if you better separate the actual results and the discussion. Some of the results section reads more like a discussion while the discussion is sometimes very technical, how do your results relate to other literature?

While we acknowledge that the paper is structured somewhat unconventionally, we believe that this format is preferable for the material we present. Because of the novel nature of our method, our results must be interpreted carefully, and so we decided that it would be helpful to provide more guidance and interpretation in the results section. As we edited the paper towards that goal, it became apparent that it would be more concise to avoid splitting topics

across the results and discussion sections. For example, we already had some examples of fire suppression in the results section to help the reader grasp "negative burned area"; it felt artificial and disjointed to then come back to that topic in the discussion section. We thus reserved the discussion section for more general treatment of concepts that arise from our results (4.1, 4.3), and for the consideration of input data quality (4.2).

All that said, the point asking for more comparison of our results with the existing literature is well taken. We will add more references to and discussion of previous work at various points throughout the Results and Discussion sections.

4.3 Impacts of regional analysis: This is an interesting discussion. Poor performance for Europe seems to be mostly a matter of Europe having many fires in all three land use classes while their spatial distribution may provide little information on the distribution of these fires. It may help to better discuss the differences in land use management between different areas. For example in Eastern Europe and Russia agricultural fires might be common practice but similar fires will not be found in Spain or Italy.

We will include more concrete examples here, citing for example the work of Lin et al. (2012; *Ecological Applications*) and Leff et al. (2004; *Global Biogeochemical Cycles*).

In a similar way, it will be hard to compare pastures across the world. Some of the grazed savannas will appear so close to natural vegetation that the a measure of "livestock density" may be more useful than "grazed or not grazed". On top of that, what about the naturally occurring herds of herbivores, especially in Africa. The FAO has published an interesting map of global livestock density.

Savannas can indeed have their fire regimes affected by heavy grazing pressure. We note, however, that what is important to our paper is isolating the effects of land management on fire. People absolutely do manage non-agricultural land, often through the use of fire and sometimes for hunting wild grazers. Understanding the regional and global scope of such management would be an interesting line of research, but is beyond the scope of this paper, where we have chosen to focus solely on lands with crops or livestock.

However, this comment gets at another important idea – how blurred the line can be between "pasture" and other land in some areas, and how that makes the FAO statistics a bit cloudy. We have already alluded to this in Section 4.2, but will some pasture-specific discussion and specific examples there.

The good performance of the model for Boreal Asia and for analysis regions where nearly all fires occur in a single land use type is obvious because the model just represents the mean values of the observations for that land use in the analysis region. The high number of analysis regions where this is the case is partly a consequence of the way the authors have defined the analysis regions in the first place. The authors should better acknowledge/discuss this. Now you state "Another, more general consequence .. in the results". Here it would really help if you would have presented how much of the spatial variation in burned area

could actually be explained by land use. And then just state something like "On average, only xx% of the spatial variation in burned area could be explained by land use, hence for many of the regions the values simply represent the mean burned area for the given land use in the analysis region." Finally, a short discussion of the alternative sources of spatial variation in burned area might be helpful.

We will add some discussion of the importance of a region including examples of grid cells with a wide range of values for each land cover type. We will also discuss the possibility that one land cover type might dominate the signal, which could for example explain the good performance for Boreal Asia in terms of total fire despite its containing several large analysis regions.

This PDF contains the marked-up version of our article. Deleted text is ~~red and stricken through~~, and inserted text is blue. Deleted figures are marked by a red border, and inserted figures by a blue border.

We wholeheartedly thank the Associate Editor and the two anonymous reviewers for their help in bringing this paper to fruition. Here is the list of changes between the initial and final version:

- Added a clause in second paragraph of Introduction.
- Cited Bistinas et al. (2013) instead of Prentice et al. (2011) in fourth paragraph of Introduction, and edited text accordingly.
- Changed $\widehat{F_{k,i}}$ symbols to $\widehat{F_k}$ in Equation 2.
- Added text and citations between Equations 4 and 5 reiterating how negative $\widehat{F_k}$ values can represent a real suppression effect.
- Added text at end of Section 2.1 paragraph beginning "Conversely,...", including a new paragraph, to try and explain more clearly what $\widehat{F_k}$ values really mean.
- Converted Appendix to Supplement, changing text throughout manuscript where necessary. Please advise on typesetting for the Supplemental Figures PDF.
- Added citations of van Der Werf et al. (2010) where appropriate to indicate that Randerson et al. (2012) used their methodology for GFED3s emissions.
- Added maps of mean land cover to Supplement.
- Added, to third paragraph of Section 3.1, results of linear regression showing how closely the total estimated burned area matches observations at the level of each month and GFED region. Also, added a figure to Supplement illustrating this.
- Reworked last paragraph of Section 3.2, mostly to incorporate comments by Paul Laris on original manuscript.

- Added, to first paragraph of Section 4.3, specific discussion of the literature regarding cropland in Europe to illustrate how a large region could have resulted in poor performance by the analysis.
- Added a paragraph after the first of Section 4.3, discussing how too-small analysis regions might affect results.
- Slightly changed last sentence of first paragraph of Conclusion.
- Added acknowledgement of Paul Laris and the referees.
- Renumbered Supplement figures to account for added figures.
- Added explanation of "Crop+" to captions of Figures 3 and S3.
- Added explanation of method used in generating Figures 4 and A5.
- Edited Figures 7 and S5: Added legend to (a), reduced white space on left side of X-axis in (b). Also edited captions.
- Edited captions of Figures 8 and S13 to make it clearer that bins are used for regressions in (b).

Manuscript prepared for Biogeosciences Discuss.
with version 2015/04/24 7.83 Copernicus papers of the LaTeX class copernicus.cls.
Date: 23 October 2015

Quantifying regional, time-varying effects of cropland and pasture on vegetation fire

S. S. Rabin[1], **B. I. Magi**[2], **E. Shevliakova**[3], **and S. W. Pacala**[1]

[1]Princeton University, Dept. of Ecology and Evolutionary Biology, Princeton, NJ, USA
[2]University of North Carolina at Charlotte, Geography and Earth Sciences Department, Charlotte, NC, USA
[3]GFDL-Princeton University Cooperative Institute for Climate Science, Princeton, NJ, USA

Correspondence to: S. S. Rabin (srabin@princeton.edu)

Abstract

The global extent of agriculture demands a thorough understanding of the ways it impacts the Earth system through both the modification of the physical and biological characteristics of the landscape as well as through emissions of greenhouse gases and aerosols. People use fire to manage cropland and pasture in many parts of the world, impacting both the timing and amount of fire. So far, much previous research into how these land uses affect fire regimes has either focused on individual small regions or global patterns at annual or decadal scales. Moreover, because pasture is not mapped globally at high resolution, the amount of fire associated with pasture has never been quantified as it has for cropland. The work presented here resolves the effects of agriculture – including pasture – on fire on a monthly basis for regions across the world, using globally gridded data on fire activity and land use at 0.25° resolution. The first global estimate of pasture-associated fire reveals that it accounts for over 40 % of annual burned area. Cropland, generally assumed to reduce fire occurrence, is shown to enhance or suppress fire at different times of year within individual regions. These results bridge important gaps in the understanding of how agriculture and associated management practices influence vegetation fire, enabling the next generation of vegetation and Earth system models more realistically incorporate these anthropogenic effects.

1 Introduction

Vegetation fire is a worldwide phenomenon with consequences for the biosphere, atmosphere, climate, and human health. Annual emissions of carbon (in various chemical forms) from fire have been estimated at 2.5 $\mathrm{Pg\,yr^{-1}}$ (2001–2009; Randerson et al., 2012). The radiative forcing from the black carbon emitted from fires since 1750 has been estimated to be 0.2 $\mathrm{W\,m^{-2}}$, which is about equivalent to 12 % of radiative forcing due to the accumulated anthropogenic CO_2 over the same time period (Bond et al., 2013; Myhre et al., 2013). Other gas and aerosol emissions from biomass burning can have notable impacts on atmo-

spheric composition and regional weather (Crutzen and Andreae, 1990; Cox et al., 2008). Many ecosystems are shaped by fire (or the lack thereof): the frequency and seasonal timing of burns are integral to what's known as a fire regime, changes to which can, over time, result in shifts to different ecosystem types (Pyne et al., 1996b; Archibald et al., 2013; Scott et al., 2014). Model simulations of an Earth without fire have resulted in about twice as much forest area (Bond et al., 2005) or nearly 30 % more carbon stored in land ecosystems (Ward et al., 2012), which illustrates the important role that fire plays in the global carbon cycle.

Humans have been manipulating fire regimes for at least several thousand years, with anthropogenic influence having grown considerably since the Industrial Revolution (Marlon et al., 2008; Bowman et al., 2011; Archibald et al., 2012). People have suppressed wildfire actively to protect lives and property, and passively by creating landscapes that inhibit large-scale fire spread. Humans have also induced burning both intentionally and unintentionally (Pyne et al., 1996a; Bowman et al., 2011). Such anthropogenic influences can result in fire regimes that differ in important ways from how ecosystems would burn in the absence of humans, such as in terms of frequency, severity, and seasonality. For example, evidence suggests that burning often does not occur during the period of the year with peak flammability, likely reflecting human fire practices at local to regional scales rather than natural or even accidental ignitions (Le Page et al., 2010; Magi et al., 2012). In order to understand the changes humanity has made to fire regimes and how patterns of vegetation fire will continue into the future, we must identify and interpret the signatures of different human activities on observed fire patterns.

One widespread example of humans' influence on fire regimes is prescribed burning for agricultural management. Farmers may use fire to prepare fields for planting or to dispose of waste after harvest (Yevich and Logan, 2003); pastoralists can burn to enhance forage nutrient content or prevent woody encroachment (Uhl and Buschbacher, 1985). The presence of cropland or heavily grazed pasture can also reduce fire in the surrounding landscape by limiting fire spread (Archibald et al., 2008; Andela and van der Werf, 2014). Land managers sometimes take advantage of a similar effect by burning small patches of land surround-

ing their property, reducing the chances that a burn could spread into their fields (Laris, 2002). Fire amplification can happen as well, with agricultural management fires spreading onto non-agricultural lands. The total worldwide influence of these and other effects of agriculture on vegetation fire is poorly understood, even though cropland and pasture respectively accounted for 11 and 24 % of the Earth's land area at the beginning of this century (Klein Goldewijk et al., 2010).

Dynamic global vegetation models and Earth system models often include process-based simulations of vegetation fires (e.g., Lenihan et al., 1998; Arora and Boer, 2005; Thonicke et al., 2010). Human influence is usually included as a function of population density (Venevsky et al., 2002; Pechony and Shindell, 2009), although some authors have noted that such relationships are ~~poorly constrained and may not be useful (Prentice et al., 2011)~~ too simplistic, with the effect of population density actually varying based on biome or amount and type of land use (Bistinas et al., 2013). Recent work has included the suppressive effect associated with cropland through landscape fragmentation (Pfeiffer et al., 2013; Le Page et al., 2015). These effects of humans in global models are based on analyses done at the scale of individual regions (e.g., Archibald et al., 2008) or the entire globe (e.g., Bistinas et al., 2014). Bistinas et al. (2014), for example, found that fire is negatively correlated with cropland but positively correlated with pasture, taking into account a number of other variables. Such findings, however, do not fully capture the complexity and multitude of effects that managed ecosystems can have on fire. It is possible, for instance, that farmers in some part of the world might burn cropland during an otherwise fire-free season, but that in drier parts of the year cropland could fragment the burnable landscape and thus have a suppressive effect on fire. Remote sensing data from satellites can partially fill in such gaps: estimates of burning on different land cover types are generated by overlaying fire activity data with maps of land use and vegetation type, including cropland, which are produced by some of the same satellites (Korontzi et al., 2006; Giglio et al., 2010). For example, such estimates were used by Li et al. (2013) to incorporate cropland burning into a global fire model. However, because pasture has not been mapped by satellite as cropland has, no global estimates of pasture burning have ever been produced. This means that estimates

of pasture and non-agricultural fire are entangled in global datasets, and thus observations have not distinguished what may be important differences in fire regime. To understand the total effect of agricultural management on fire occurrence, then, the scientific community must go beyond estimates of cropland burned area and associated emissions.

The work presented here is an effort to bridge these gaps in our knowledge. We present a method that uses fire observations in conjunction with estimates of land-use distribution to statistically estimate the amount of fire associated with cropland, pasture, and other lands at global and regional scales. In addition to examining the total area of such burning, the same method is used to investigate patterns of associated carbon emissions.

2 Methods

2.1 Analytical technique

Magi et al. (2012) analyzed seasonal patterns of agricultural burning (i.e., combined cropland and pasture) from non-agricultural burning using estimates of land-use distributions and satellite-derived fire data. This study builds upon the methods presented by Magi et al. (2012), differentiating among cropland, pasture, and other burning and generating estimates of the amount of each type of fire in terms of both burned area and carbon emissions.

The total amount of burned area in some grid cell i (B_i) can be represented as the sum of the burned area on each land-use type k. This can in turn be represented as the product of the area of that land cover type in the grid cell ($A_{k,i}$) and the fraction of that land-use type that burned in that grid cell ($F_{k,i}$):

$$B_i = F_{\mathrm{c},i}A_{\mathrm{c},i} + F_{\mathrm{p},i}A_{\mathrm{p},i} + F_{\mathrm{o},i}A_{\mathrm{o},i} \quad (1)$$

where the subscripts c, p, and o refer to cropland, pasture, and other land, respectively. The values of each $F_{k,i}$ are unknown, but a best-guess $\widehat{F_k}$ can be estimated across a group of

N grid cells:

$$\begin{bmatrix} B_1 \\ B_2 \\ \vdots \\ B_i \\ \vdots \\ B_N \end{bmatrix} = \begin{bmatrix} A_{c1} & A_{p1} & A_{o1} \\ A_{c2} & A_{p2} & A_{o2} \\ \vdots & \vdots & \vdots \\ A_{ci} & A_{pi} & A_{oi} \\ \vdots & \vdots & \vdots \\ A_{cN} & A_{pN} & A_{oN} \end{bmatrix} \times \begin{bmatrix} \widehat{F_{\mathrm{c},i}} \\ \widehat{F_{\mathrm{p},i}} \\ \widehat{F_{\mathrm{o},i}} \end{bmatrix} + \begin{bmatrix} \epsilon_1 \\ \epsilon_2 \\ \vdots \\ \epsilon_i \\ \vdots \\ \epsilon_N \end{bmatrix} \tag{2}$$

$$\boldsymbol{B} = \mathbf{A}\widehat{\boldsymbol{F}} + \boldsymbol{\epsilon} \tag{3}$$

where ϵ_i is the residual for grid cell i. The set of $\widehat{F_k}$ values that minimize the sum of squared errors across a large number of grid cells can be calculated using

$$\widehat{\boldsymbol{F}} = (\mathbf{A}^\intercal \mathbf{A})^{-1} \mathbf{A}^\intercal \boldsymbol{B} \tag{4}$$

where $\mathbf{A}$ and $\boldsymbol{B}$ are observations of land-use distributions and burned area, respectively. We have observed that a number of $\widehat{F_k}$ values are found to be negative. This has two possible interpretations. One is that negative $\widehat{F_k}$ values are simply a statistical artifact of the analysis without physical meaning, and that such lands either burn very little or not at all. The other possibility is that negative $\widehat{F_k}$ values represent a real aspect of fire occurrence: namely, that the negative influence of such land covers on other land covers outweighs any fire happening on the land cover itself. This could be considered to represent either active suppression to protect high-value land such as crop fields, and/or to reflect the widely-documented role of anthropogenic land covers (especially cropland) in fragmenting the burnable landscape (Archibald et al., 2008; Andela and van der Werf, 2014; Hantson et al., 2015).

For the purposes of illustration, consider a hypothetical grid cell for which the analysis estimates 5 km^2 of burned area for cropland:

$$F_{\mathrm{c},i} A_{\mathrm{c},i} = 5 \tag{5}$$

$$B_i = F_{\mathrm{c},i}A_{\mathrm{c},i} + F_{\mathrm{p},i}A_{\mathrm{p},i} + F_{\mathrm{o},i}A_{\mathrm{o},i} \quad (6)$$

A different grid cell with equal $\widehat{F_k}$ values and twice the area of cropland but the same amounts of pasture and other land would have 5 km^2 more burning estimated:

$$F_{\mathrm{c},i}(2A_{\mathrm{c},i}) + F_{\mathrm{p},i}A_{\mathrm{p},i} + F_{\mathrm{o},i}A_{\mathrm{o},i} = B_i + F_{\mathrm{c},i}A_{\mathrm{c},i} = B_i + 5 \quad (7)$$

The same logic shows that there would be less fire in the second grid cell if $\widehat{F_{\mathrm{c}}}$ were negative.

Conversely, $\widehat{F_k}$ values could also incorporate positive effects of one land-use type on the others. For example, much of the fire observed in the frontier of the Amazon rainforest is associated with land management burning that escapes into surrounding forest (Uhl and Buschbacher, 1985; Cochrane and Schulze, 1998). The $\widehat{F_{\mathrm{c}}}$ and $\widehat{F_{\mathrm{p}}}$ values in that region could potentially account for this effect as well. In this conceptualization, then, $\widehat{F_k}$ values should be interpreted not as "the fraction of land use k that burns across the region," but rather as "the net effect of land use k on fire in the region, expressed as a fraction of the area of land use k in the region." That is, for every additional unit area of land use k, we expect $\widehat{F_k}$ more (if $\widehat{F_k} > 0$) or fewer (if $\widehat{F_k} < 0$) units of burning.

To clarify, imagine a region with 2,000 km^2 of cropland, 3,000 km^2 of pasture, and 5,000 km^2 of other land. For some month, this region has $\widehat{F_c} = -0.1$, $\widehat{F_p} = 0.2$, and $\widehat{F_o} = 0.1$. The associated burned area values would be $2000 \times -0.1 = -200\ \mathrm{km}^2$ for cropland, $3000 \times 0.2 = 600\ \mathrm{km}^2$ for pasture, and $5000 \times 0.1 = 500\ \mathrm{km}^2$ for other land, for a total of 900 km^2 of burning across the region. Now imagine another region that is identical except that it contains an extra 1,000 km^2 of cropland. This new region would have $3000 \times -0.1 = -300\ \mathrm{km}^2$ of burned area associated with cropland, for a total of 800 km^2 of burning across the region. The interpretation of negative cropland-associated burned area is not that some actual negative area is burning somehow, but rather that however much cropland is burning, it is preventing so much fire on pasture and/or other land that its net influence on fire in the region is negative.

The results presented in this study are explored in the main text with this latter interpretation of $\widehat{F_k}$ values in mind. ~~Appendix A~~ Equivalent figures in the Supplement show~~s~~ results with $\widehat{F_k}$ restricted to positive values, essentially interpreting $\widehat{F_k}$ values as "the fraction of land use k that burns across the region."

To account for temporal variability in the total amount of fire and its distribution among different land-use types, the analysis is performed separately for each month and year. Fire patterns and practices also vary across space, so each of 132 regions is analyzed separately. This set of regions (Fig. 1) was created with the goal of minimizing within-region heterogeneity in terms of climate, biome, and fire extent and timing, while still including enough grid cells to ensure an adequate sample size for estimation. The final region set resulted from an iterative process whereby we performed the analysis for a candidate region set, noted areas of severe under- or over-estimation, drew new region boundaries, and re-ran the analysis. The Terrestrial Ecosystems of the World map (Olson et al., 2001), agricultural distribution maps (Klein Goldewijk et al., 2010), and observations of fire extent and timing (Randerson et al., 2012) guided development of the regions map. For example, regions were designed to avoid containing multiple patches of high concentration of a land use that appeared to vary widely in seasonal timing or amount of fire. As in Magi et al. (2012), the fourteen regions developed for the Global Fire Emissions Database (Giglio et al., 2006) are used to structure the discussion of the results presented here (Fig. 1, Table 1). For clarity, these will be referred to as the "GFED regions," to distinguish them from the 132 "analysis regions." In all, 4752 $\widehat{F_k}$ values are estimated per year (3 land-use types $\times$ 12 months $\times$ 132 analysis regions) from 2001–2009. A shapefile containing the analysis regions for use in GIS software can be found in the Supplement file.

Some restrictions were imposed on the analysis. Any land-use type whose prevalence across a region during a given year was on average less than 5 % was excluded, with the $\widehat{F_k}$ value for such land cover types taken to be zero, to avoid issues of near-singularity in the matrix calculations. Also, for region-months with no observed fire, all $\widehat{F_k}$ values were assumed to be zero.

2.2 Input data

2.2.1 Burned area and fire emissions

Observations of monthly burned area and carbon emissions at 0.25° resolution were obtained from the GFED3s dataset (Randerson et al., 2012). Based on the Global Fire Emissions Database version 3 ~~(GFED3; Giglio et al., 2010)~~ (GFED3; Giglio et al., 2010; van der Werf et al., 2010), GFED3s was designed to improve detection of small fires by incorporating an estimate of burned area based on detections of active fires outside observed fire scars. This algorithm produces an estimate of annual burned area 35 % higher than the Collection 5 MCD64A1 burned area product, which was produced using the same algorithm as most of the GFED3 data, across the time period of its coverage (2001–2010), with several large regions seeing their burned area estimates more than double (Randerson et al., 2012). Nearly a fifth of that increase occurred in croplands and cropland/natural vegetation mosaic, the estimated burned area of which increased by 123 and 79 %, respectively. Moreover, about a third occurred in savannas and grasslands, which could feasibly serve as pasture (Randerson et al., 2012). Results for cropland influence on burned area from this analysis are compared to GFED3s estimates of burned area on cropland as well as "cropland-natural mosaic," which is defined as land with "a mosaic of croplands, forests, shrubland, and grasslands in which no one component comprises more than 60 % of the landscape" (Friedl et al., 2002).

GFED3s estimates of fire-related emissions were generated, as for the original GFED3 dataset (van der Werf et al., 2010), by coupling the burned area observations for each land-use type with a climate-driven vegetation model (Randerson et al., 2012). Biome-specific emissions factors combined with biomass estimates from the vegetation model then produced the amount of emissions per area burned. The analytical technique described in Sect. 2.1 can be as easily applied to emissions as it can to burned area, in which case the $\widehat{F_k}$ values represent the net effect per square kilometer of each land-use type on fire emissions. Here, an analysis of emissions of carbon-containing compounds was conducted

in parallel with the analysis of burned area. A breakdown of GFED3s carbon emissions by land cover type, such as was provided for burned area, was not available.

2.2.2 Land use

Data on area of cropland and pasture were taken from an annualized version of the History Database of the Global Environment version 3.1 (HYDEv3.1), described by Klein Goldewijk et al. (2010). This public dataset, available at 5 min spatial resolution, is the basis for the historical part of the standardized gridded land-use transitions reconstructions (Hurtt et al., 2011) used in the Coupled Model Intercomparison Project, phase 5 (Taylor et al., 2012). The publicly available data are only produced for every five years during the recent past, but K. Klein Goldewijk provided annual estimates for the period 2000–2009 (personal communication, 2012). Distributions are assumed to not change within years. The amount of "other" ("non-agricultural") land is calculated as the fraction of land not classified as cropland or pasture. Maps of the mean land cover distributions from HYDE for 2001–2009 can be found in Fig. S1.

Grazing land can take many different forms, including both planted forage species and naturally occurring species (often referred to as rangeland). Data from the Food and Agriculture Organization (FAO) were used in compiling maps of present-day land use in HYDE; HYDE's pasture data is based on the FAO's "permanent meadows and pastures" (Klein Goldewijk et al., 2007). These are defined as lands "used permanently (five years or more) to grow herbaceous forage crops, either cultivated or growing wild (wild prairie or grazing land)" (FAO, 2005). The term "pasture" is thus used throughout this paper in this broad land-use sense. Note, however, that this is distinct from any given land cover type, such as grassland or savanna – that is, all pasture has herbaceous vegetation, but not all land with herbaceous vegetation is necessarily pasture.

2.2.3 Spatiotemporal coverage and resolution

All analyses were performed at the native resolution of GFED3s, 0.25°, with HYDE land-use data being downscaled to match. The analysis covered the period 2001–2009, as HYDE data for 2010 were not available.

3 Results

3.1 Fire extent

Every year, nearly half of all burned area is associated with agricultural lands (Fig. 2a): pasture contributes 203 $\mathrm{Mha\,yr^{-1}}$ of burned area, while cropland accounts for 21 $\mathrm{Mha\,yr^{-1}}$. Non-agricultural lands are associated with 243 $\mathrm{Mha\,yr^{-1}}$ of burned area. Overall, the analysis slightly overestimated total global annual burned area, giving 467.6 $\mathrm{Mha\,yr^{-1}}$ instead of 466.9 $\mathrm{Mha\,yr^{-1}}$ (+0.2 % error).

The distribution of fire emissions across land-use types differs strongly from what might be expected based on their relative burned areas. Whereas annual burned area associated with non-agricultural land was only $\sim 20\,\%$ greater than that with pasture, non-agricultural land was responsible for over 260 % more fire C emissions (Fig. 2b). Emissions per area burned can be thought of as the product of fuel load and combustion completeness – i.e., the amount of dead and living biomass multiplied by the fraction combusted (Seiler and Crutzen, 1980). Fuel load should be higher on average for non-agricultural lands than for pasture because pastures do not have trees in densities comparable to more carbon-rich forest ecosystems. Moreover, although croplands had a net positive contribution to global burned area, they had a net negative effect on fire emissions (Fig. 2). This suggests that, even though less area would have burned with less cropland, the burning would be happening in more carbon-dense ecosystems. As with burned area, total global fire emissions were very slightly overestimated (by less than 0.4 %; Fig. 2b).

Figure 3 shows time series plots as in Fig. 2, but broken down by GFED region. Pasture can be seen to account for a sizable portion of burning in South America (NHSA and SHSA), Africa (NHAF and SHAF), Central Asia (CEAS), and Australia (AUST). Overall, the algorithm reproduces the amount and interannual variability of total fire well at these large regional scales: On a scatter plot comparing the estimated and observed burned area of the 1,512 GFED region-months (14 regions $\times$ 108 months), most points fall near the one-to-one line (linear regression y-intercept $= -3.7 \times 10^{-3}$, slope $= 1.0008$, Pearson's $r = 0.9997$; Fig. S4). The most apparent discrepancies compared to GFED3s occur in Europe (EURO) and the Middle East (MIDE), whose mean annual burned area totals are underestimated by ~ 40 and $\sim 30\,\%$, respectively. With respective mean annual observed burned areas of $\sim 11\,200$ and $\sim 15\,800\,\mathrm{km}^2$ (0.2 and 0.3 % of global fire activity), however, these are the least-burned GFED regions.

The net mean annual burned area associated with croplands, pasture, and other land is illustrated in the maps in Fig. 4. Pasture accounts for a large amount of burned area in the savannas of NHAF and SHAF, with NHSA, SHSA, CEAS, and AUST being highlighted to a lesser degree. Eastern Europe, northern Australia, various parts of sub-Saharan Africa, and especially India's Punjab state emerge as spots where cropland has a strong positive effect on burned area (Fig. 4a). Cropland has a net negative effect on burned area in other places – most notably Cambodia and southern Vietnam, Ethiopia and South Sudan, India, eastern Argentina, and southeastern Australia. These are mostly biomes where vegetation tends to be quite fire-prone, and thus where strong active and/or passive suppression due to cropland might be expected. Interestingly, pasture and non-agricultural lands are also seen to sometimes have net suppressive effects (Fig. 4b and c). In the case of pasture, this could be due to a passive effect – grazing pressure can reduce fuel loads, leading to slower-spreading and/or less-frequent fires (Cheney and Sullivan, 2009). Non-agricultural lands with net negative influence may result from either active or passive suppression. People might use alternative management techniques to avoid fire use on cropland or pasture near valuable or protected forests, for example. Alternatively, if fire on pasture is at least to some extent unmanaged, less-flammable vegetation types such as forest or wetland could serve

to break up pasture into disconnected patches and thus reduce how much it can burn. It is also important to remember that apparent negative influences might not represent any real process, being instead artifacts of this analysis (~~Appendix A~~ see figures in Supplement). Overall, the algorithm generates maps of total fire that broadly agree with the distribution of burning seen in the observations (Fig. 5). However, the spatial variation in burned area within regions is not fully captured; we discuss this further in Section 4.3.

3.2 Fire timing

The previous results have shown the influence of different land-use types on fire at an annual level, but land use and management can also affect the seasonality of fire. Figure 6 shows, for each GFED region, the mean seasonality of estimated and observed burned area and carbon emissions as compared with observations. As expected based on the algorithm's performance with regard to annual total fire (Fig. 3), all regions except EURO and MIDE show good correspondence between observations and estimates of total fire.

Estimated cropland fire is sometimes higher or lower than GFED3s for cropland or cropland-natural mosaic. One reason for this is that the analysis may describe the net effect of cropland on fire, as discussed above. Another is that detection of cropland, especially of small fields, is difficult using moderate-resolution satellite imagery, such as the MODIS MCD12 dataset used in GFED3s (Friedl et al., 2010). Klein Goldewijk et al. (2007) for example, had to deal with this in developing HYDE. In some regions – such as the contiguous 48 US (a.k.a. Temperate North America, TENA), Europe (EURO), and Central Asia (CEAS) – trends of estimated cropland burned area closely follow those from observations (Fig. 6). In other regions – such as Northern Hemisphere South America (NHSA) and Equatorial Asia (EQAS) – cropland has an apparent negative influence on burned area for several months of the year. A comparison with observed cropland burning (of which there is little in such months) suggests that this is often a nearly pure signal of a suppressive effect. The effect appears especially strong in EQAS during September and October, although the large amount of cropland-natural mosaic burning complicates interpretation there. Pasture sometimes has a similar effect, although rarely; this is most apparent in TENA, EURO, MIDE, and

SEAS. In EURO and CEAS, even other lands sometimes have a net negative estimated burned area. As discussed above, negative influence of pasture and non-agricultural lands could reflect active and/or suppressive effects associated with these land use/cover types.

Figures S8–S11 present another way to examine the seasonal changes in the influence of different land covers on burning. This presents an advantage over the regional timeseries discussed above where contrasting patterns exist within one GFED region. For example, Figure S9a shows that cropland is contributing to burned area in southwestern Australia from March to May, but is suppressing fire in the northern part of the continent. Figure 6 does not capture this pattern, instead making it appear as though cropland has no effect across the entire region of Australia and New Zealand (AUST).

The effect of different land uses on fire can be best explored and understood by examining patterns across a few regions. The savannas of western Africa have seen a good deal of remote sensing, anthropological, and ecological research regarding their fire regimes and thus provide a good example. The Sudanian savanna there experiences a distinct dry season from approximately October or November through April or May, during which it burns extensively (Laris, 2002; Kull and Laris, 2009). The fire regime is highly managed by people for agriculture and other purposes, with burning generally initiated early in the dry season and suppressed later. Early fires can have a number of benefits. For example, burning that occurs while the soil still has some residual moisture allows herbaceous regrowth, replenishing food availability for livestock ahead of the worst of the dry season (Mbow et al., 2000). Due to higher fuel moisture, these fires are also often easier to control than more intense burns under more flammable conditions later in the dry season. People often burn savanna early to fragment the burnable landscape, preventing late-season burns that can damage property and resources (Laris, 2002).

We isolated three regions (Fig. 7a) that mostly fall into the ecoregions “West Sudanian savanna” and “Guinean forest-savanna mosaic” according to Olson et al. (2001). Small amounts of other land cover types – including lowland and montane forests, flooded savanna, and Sahelian acacia savanna – are also included. On average, this area sees a slight negative annual contribution of cropland to burned area~~;~~ – that is, cropland tends to reduce

the amount of burning on pasture and other lands. Pasture contributes over a third of the observed annual burned area, with non-agricultural lands accounting for approximately twice that. Observed total burned area, which is matched almost perfectly by the estimate, peaks with pasture and non-agricultural burning in December (Fig. 7). As expected based on the literature on human fire management practices in this region (Mbow et al., 2000; Laris, 2002), most fire associated with pasture and non-agricultural land occurs in the early dry season – i.e., before January. Interestingly, though, the fire season for pasture seems to begin and end about a month earlier than that of non-agricultural land: from about October through January instead of November through February. Although early fire is often beneficial for all savanna in the region, the added impetus of burning early to create food for livestock appears to result in a distinct pattern. However, it is also possible that the October burning represents intentional burning of short-grass savanna, which is not actually used by livestock but may have been considered "pasture" in the land use data (P. Laris, personal communication, 2015). An overall net suppressive effect of cropland is also evident~~, with the~~. The strongest negative influence correspond~~,ing to~~s with both the December peak of non-cropland fire and the harvest (P. Laris, personal communication, 2015; Figs. 7b, S8–S11). This emerges despite the fact that at least some cropland burning (including cropland-natural mosaic) was observed throughout the dry season (Fig. 7b). Even though there is some observed fire associated with cropland, then, there would be much more if cropland were replaced with pasture or non-agricultural land. This interpretation has assumed that negative values are meaningful, but similar patterns emerge using constrained $\widehat{F_k}$ values (Fig. ~~A6~~S12).

4 Discussion

4.1 First estimates of pasture-associated fire

Pasture fire accounts for about 43 % of global annual burned area and about 22 % of global C emissions from fire. Pasture burning is especially important in CEAS, NHSA, NHAF,

SHAF, and SHSA, in each of which it accounts for over 40 % of annual burned area. These regions together comprise 81 % of mean annual burning. As with the global numbers, the fraction of annual fire emissions from pasture burning there is disproportionately small – only NHSA has pasture contributing more than 40 % of C emissions (Fig. 3b). These results are not qualitatively different in the analysis with $\widehat{F_k}$ values constrained to zero or above (Appendix A).

In most regions, the seasonality of pasture burning is roughly similar to that of non-agricultural land. A tendency for pasture to burn earlier than non-agricultural land is apparent in NHSA, EURO, MIDE, NHAF, SEAS, and to some extent AUST (Fig. 6). The seasonality of these two fire types is notably different in CEAS, where pasture fire peaks in August and non-agricultural fire peaks in May. During the peak of pasture burning in that region, non-agricultural land exerts a negative influence on total burning (Fig. 6). Some insight into the interplay of the different land-use types in this region, as well as the intricacies involved in interpreting the estimates from our method, can be gleaned from a more detailed look at pasture and other fire in CEAS. Most of the negative influence of non-agricultural land is concentrated in northern Kazakhstan and surrounding Russia. This is also the sub-region where most pasture fire is concentrated during its July–August–September peak, which corresponds to the strongest negative influence of non-agricultural land. Taken together, these details suggest that there is at least some uncontrolled burning happening on pasture there at that time, since the presence of other land (presumably less-flammable vegetation types such as forest) appears to reduce pasture fire, likely by fragmenting the burnable landscape.

4.2 Input data quality

As with all data analysis, the performance of this algorithm is restricted by how well its input data represent the real world. Errors in the datasets of either land use or burned area will propagate through to the $\widehat{F_k}$ estimates and partitioned maps of fire by land-use type.

The first step in the development of the HYDE land-use dataset was the production of a map of cropland and pasture representative of their distribution during the period 1990–2000. By reconciling remote-sensing maps of land cover with country-level area totals from

the Food and Agriculture Organization (FAO), HYDE represented a significant advance over previous methods (Klein Goldewijk et al., 2007, 2010). However, the FAO numbers themselves may not be completely internally consistent, since they are compiled and reported by each country. A wide variety of ecosystem types and land-use patterns might all qualify as what the FAO terms "permanent pasture," and countries' standards of what to report likely differ (Klein Goldewijk et al., 2007). Differing methods of compilation introduce another source of uncertainty.

By incorporating active fire detections as an ancillary source of "burned area" information, the algorithm used in GFED3s was designed to avoid (as much as possible) the issue of fires much smaller than a single sensor pixel being excluded (Randerson et al., 2012). Even though GFED3s includes much more cropland fire than GFED3, it likely still misses much such burning. For example, McCarty et al. (2009) used fieldwork to inform a remote sensing estimate of cropland burning in the contiguous US and found that an average of more than 1.2 $\mathrm{Mha\,yr^{-1}}$ burned between 2003 and 2007; during the same period, GFED3s has only 0.67 $\mathrm{Mha\,yr^{-1}}$ (or 0.93 $\mathrm{Mha\,yr^{-1}}$ if also including cropland-natural mosaic). Moreover, the "small fires" improvement may not have improved the detection of burning underneath a relatively undamaged canopy, which poses a challenge even for active fire sensors and algorithms (Giglio, 2013). In regions of southern Africa with tree cover $\geq 21\,\%$, this was blamed for a 41 % underestimate of burned area in an assessment of the algorithm underlying most of GFED3 (Giglio et al., 2009); a similar assessment has not been performed for GFED3s.

4.3 Impacts of regional analysis

The specific set of regions chosen for this analysis can be important for the quality of the results. One aspect to consider is that analysis regions that are too extensive may encompass too many different fire patterns for any one set of $\widehat{F_k}$ values to describe well. This may have been the cause of the poor performance in EURO and MIDE with regard to total fire (Fig. 3): both include parts of one or more very large analysis regions (Fig. 1). Fire is much more frequently used to manage croplands in the eastern part of the large EURO analysis

region than in the west (Lin et al., 2012). This could be due to different crops being grown, but this seems unlikely since wheat and maize comprise most of the cropland across the region (Leff al., 2004). Instead, differences in cultural history, policies regulating residue burning, and economic conditions probably play a large role. Breaking the large region into more fine-grained regions would likely better account for this heterogeneity in fire patterns and practices.

~~Large analysis regions are not necessarily detrimental, however – Boreal Asia (BOAS) has several (Fig. 1) but is relatively well described (Fig. 3).~~ On the other hand, analysis regions that are too small – specifically, that do not sample grid cells with a wide range of values for each land cover type – may serve to confound the results. In an extreme example, a region that had no cropland would be assigned $\widehat{F_c} = 0$. However, because no cropland was observed, the true effect cropland would have in the region might actually be different from zero. In a less extreme case, burning patterns might be controlled mostly by the influence of one dominant land cover type. This sort of effect could be at play in BOAS, for example, where (as discussed above) total regional burned area is estimated accurately despite its containing several large regions.

Another, more general consequence of the regional analysis is that spatial heterogeneity of burning within analysis regions is not well represented in the results. As expected based on the mathematics involved in the parameterization, the total estimated amount of fire at the regional level is usually quite accurate (Fig. 8a) – estimated total burned area was correct to within 5 % in 86 % of region-months with fire observed. A best-fit line through a plot of the total observed vs. estimated burned area of all region-months illustrates this. With a slope near one, intercept near zero, and high value of Pearson's r, most of the estimated means lie near the one-to-one line. On a finer-grained level, a best-fit line through the mean estimated burned area of bins of gridcell-level observed burned area, equally spaced on a log scale, shows that the algorithm tends to overestimate burning where there is little observed fire and underestimate where observed burning is high (Fig. 8b), but the scatter of individual grid cells around these binned averages is large. Especially noticeable is the large number of grid cells with zero (or very little) observed fire that are overestimated by the al-

gorithm. When calculated across all gridcells in all months, the coefficient of determination $R^2 = 0.356$, indicating that only just over a third of the variation in spatiotemporal patterns of fire can be explained by land-use distributions. More of the variability is due to factors governing fuel availability and moisture, such as net primary productivity, temperature, precipitation, and humidity (Bistinas et al., 2014; Lasslop et al., 2015). In region-months where land cover distributions have very low explanatory power, the individual $\widehat{F_k}$ values should tend towards the total fraction of land burned.

The maps in Fig. 5 illustrate this problem in a more intuitive format. Although fire activity is usually well characterized at the level of the analysis region (as illustrated by Fig. 8a), Figure 5 shows that it does not fully incorporate the heterogeneity evident in the observations as illustrated by Fig. 8b). Thus, interpretations of the maps in Fig. 4 should focus on general patterns without delving too deeply into gridcell-by-gridcell variation.

Finally, because the GFED region boundaries do not all correspond to those of the analysis regions, GFED regions without much fire are highly sensitive to inclusion of parts of analysis regions with too much or too little estimated fire. This also may have contributed to the poor performance in EURO and MIDE (Fig. 3). For example, Afghanistan (MIDE) is included in analysis region 26, "West-central Asian desert steppe" (AR26), which is not completely contained by MIDE. Afghanistan is an area of overestimate in AR26, and although it is balanced out by underestimates elsewhere in that region (especially along its northern boundary), MIDE only includes the overestimate. This effect, then, contributes to the net overestimate in MIDE.

5 Conclusions

The analysis presented here shows that agriculture does have far-reaching consequences on vegetation fire, often in ways not previously measured or considered at large scales. The widely acknowledged suppressive effect of cropland (Archibald et al., 2008; Andela and van der Werf, 2014) is quantified by broadening the scope of land use associations with burning to include fire prevented on other land-use types. Pasture, previously not con-

sidered as a distinct land-use type in estimates of fire activity since it is not mapped globally at high resolution, is shown to account for nearly half of global annual burned area (Fig. 2a). Importantly, analysis at the regional and monthly level elucidates for the first time variations in management practices and other patterns across space and time. For example, although cropland has a net suppressive effect in parts of the world such as Southeast Asia, it enhances fire activity in regions such as southern Mexico (Fig. 4a). Even within a given region, such as ~~Mali~~ the one examined in western Africa (Fig. 7), cropland can have either an enhancing or suppressive effect on fire, depending on the time of year (Figs. ~~7b,~~ 6, S8–S11).

These new estimates of burning associated with cropland, pasture, and other land could be used for a variety of purposes. For example, a lack of data has contributed to cropland and pasture management burning being mostly ignored in global fire models (although see Li et al., 2013; Pfeiffer et al., 2013); the results from this work could inform the development of mechanisms to account for such practices. Future development of this algorithm could add terms to explicitly account for interactions between land uses, such as cropland suppressing fire on non-agricultural land. This would generate estimates of burning on cropland separate from its effect on other land-use types, further improving the utility of the results.

Appendix A: ~~Figures from constrained-~~ $\widehat{F_k}$ ~~analysis~~

~~See figures.~~

Acknowledgements. The authors would like to acknowledge funding for this work from the Carbon Mitigation Initiative, as well as a National Science Foundation Graduate Research Fellowship award to SSR. BIM was partially supported by NSF grant BCS-1436496. We also thank Kees Klein Goldewijk for sharing annual HYDE data, and James Randerson for granting early access to the GFED3s dataset. Finally, we thank Paul Laris and the two anonymous referees for valuable feedback that improved this paper.

References

Andela, N. and van der Werf, G. R.: Recent trends in African fires driven by cropland expansion and El Niño to La Niña transition, Nature Climate Change, 4, 791–795, 2014.

Archibald, S., Roy, D. P., van Wilgen, B. W., and Scholes, R.: What limits fire? An examination of drivers of burnt area in Southern Africa, Glob. Change Biol., 15, 613–630, 2008.

Archibald, S., Staver, A. C., and Levin, S. A.: Evolution of human-driven fire regimes in Africa, P. Natl. Acad. Sci. USA, 109, 847–852, 2012.

Archibald, S., Lehmann, C. E. R., Gomez-Dans, J. L., and Bradstock, R. A.: Defining pyromes and global syndromes of fire regimes, P. Natl. Acad. Sci. USA, 110, 6442–6447, 2013.

Arora, V. K. and Boer, G.: Fire as an interactive component of dynamic vegetation models, J. Geophys. Res., 110, 1–20, 2005.

Bistinas, I., Oom, D., Sá, A. C. L., Harrison, S. P., Prentice, I. C., and Pereira, J. M. C.: Relationships between human population density and burned area at continental and global scales, PLoS One, 8, e81188, doi:10.1371/journal.pone.0081188.t003, 2013.

Bistinas, I., Harrison, S. P., Prentice, I. C., and Pereira, J. M. C.: Causal relationships versus emergent patterns in the global controls of fire frequency, Biogeosciences, 11, 5087–5101, doi:10.5194/bg-11-5087-2014, 2014.

Bond, T. C., Doherty, S. J., Fahey, D. W., Forster, P. M., Berntsen, T., DeAngelo, B. J., Flanner, M. G., Ghan, S., Kärcher, B., Koch, D., Kinne, S., Kondo, Y., Quinn, P. K., Sarofim, M. C., Schultz, M. G., Schulz, M., Venkataraman, C., Zhang, H., Zhang, S., Bellouin, N., Guttikunda, S. K., Hopke, P. K., Jacobson, M. Z., Kaiser, J. W., Klimont, Z., Lohmann, U., Schwarz, J. P., Shindell, D. T., Storelvmo, T., Warren, S. G., and Zender, C. S.: Bounding the role of black carbon in the climate system: a scientific assessment, J. Geophys. Res.-Atmos., 118, 5380–5552, 2013.

Bond, W. J., Woodward, F. I., and Midgley, G. F.: The global distribution of ecosystems in a world without fire, New Phytol., 165, 525–538, 2005.

Bowman, D. M. J. S., Balch, J. K., Artaxo, P., Bond, W. J., Cochrane, M. A., D'antonio, C. M., DeFries, R., Johnston, F. H., Keeley, J. E., and Krawchuk, M. A.: The human dimension of fire regimes on Earth, J. Biogeogr., 38, 2223–2236, 2011.

Cheney, P. and Sullivan, A.: Grassfires: Fuel, Weather and Fire Behaviour, 2nd edn., CSIRO Publishing, Collingwood, Victoria, Australia, 2009.

Cochrane, M. A. and Schulze, M. D.: Forest fires in the Brazilian Amazon, Conserv. Biol., 12, 948–950, 1998.

Cox, P. M., Harris, P. P., Huntingford, C., Betts, R. A., Collins, M., Jones, C. D., Jupp, T. E., Marengo, J. A., and Nobre, C. A.: Increasing risk of Amazonian drought due to decreasing aerosol pollution, Nature, 453, 212–215, 2008.

Crutzen, P. J. and Andreae, M. O.: Biomass burning in the tropics: impact on atmospheric chemistry and biogeochemical cycles, Science, 250, 1669–1678, 1990.

FAO: Concepts and Definitions, available at: http://faostat.fao.org/site/375/default.aspx, 2005, last access: 18 June 2015.

Friedl, M., McIver, D., Hodges, J., Zhang, X., Muchoney, D., Strahler, A., Woodcock, C., Gopal, S., Schneider, A., Cooper, A., Baccini, A., Gao, F., and Schaaf, C.: Global land cover mapping from MODIS: algorithms and early results, Remote Sens. Environ., 83, 287–302, 2002.

Friedl, M. A., Sulla-Menashe, D., Tan, B., Schneider, A., Ramankutty, N., Sibley, A., and Huang, X.: MODIS Collection 5 global land cover: algorithm refinements and characterization of new datasets, Remote Sens. Environ., 114, 168–182, 2010.

Giglio, L.: MODIS Collection 5 Active Fire Product User's Guide Version 2.5, available at: https://earthdata.nasa.gov/files/MODIS_Fire_Users_Guide_2.5.pdf, 2013, last access: 18 June 2015.

Giglio, L., van der Werf, G. R., Randerson, J. T., Collatz, G. J., and Kasibhatla, P.: Global estimation of burned area using MODIS active fire observations, Atmos. Chem. Phys., 6, 957–974, doi:10.5194/acp-6-957-2006, 2006.

Giglio, L., Loboda, T., Roy, D. P., Quayle, B., and Justice, C. O.: An active-fire based burned area mapping algorithm for the MODIS sensor, Remote Sens. Environ., 113, 408–420, 2009.

Giglio, L., Randerson, J. T., van der Werf, G. R., Kasibhatla, P. S., Collatz, G. J., Morton, D. C., and DeFries, R. S.: Assessing variability and long-term trends in burned area by merging multiple satellite fire products, Biogeosciences, 7, 1171–1186, doi:10.5194/bg-7-1171-2010, 2010.

Hantson, S., Lasslop, G., Kloster, S., and Chuvieco, E.: Anthropogenic effects on global mean fire size, Int. J. Wildland Fire, 24, 589–596, doi:10.1071/WF14208, 2010.

Hurtt, G. C., Chini, L. P., Frolking, S., Betts, R. A., Feddema, J., Fischer, G., Fisk, J. P., Hibbard, K., Houghton, R. A., Janetos, A., Jones, C. D., Kindermann, G., Kinoshita, T., Klein Goldewijk, K., Riahi, K., Shevliakova, E., Smith, S., Stehfest, E., Thomson, A., Thornton, P., van Vuuren, D. P., and Wang, Y. P.: Harmonization of land-use scenarios for the period 1500–2100: 600 years of global gridded annual land-use transitions, wood harvest, and resulting secondary lands, Climatic Change, 109, 117–161, 2011.

Klein Goldewijk, K., van Drecht, G., and Bouwman, A. F.: Mapping contemporary global cropland and grassland distributions on a 5x5 minute resolution, Journal of Land Use Science, 2, 167–190, 2007.

Klein Goldewijk, K., Beusen, A., Van Drecht, G., and De Vos, M.: The HYDE 3.1 spatially explicit database of human-induced global land-use change over the past 12,000 years, Global Ecol. Biogeogr., 20, 73–86, 2010.

Korontzi, S., McCarty, J., Loboda, T., Kumar, S., and Justice, C.: Global distribution of agricultural fires in croplands from 3 years of Moderate Resolution Imaging Spectroradiometer (MODIS) data, Global Biogeochem. Cy., 20, GB2021, doi:10.1029/2005GB002529, 2006.

Laris, P.: Burning the seasonal mosaic: preventative burning strategies in the wooded savanna of southern Mali, Hum. Ecol., 30, 155–186, 2002.

Lasslop, G., Hantson, S., and Kloster, S.: Influence of wind speed on the global variability of burned fraction: a global fire model's perspective, Int. J. Wildland Fire, 22, 959–969, 2015.

Le Page, Y., Oom, D., Silva, J. M. N., Jönsson, P., and Pereira, J. M. C.: Seasonality of vegetation fires as modified by human action: observing the deviation from eco-climatic fire regimes, Global Ecol. Biogeogr., 19, 575–588, 2010.

Le Page, Y., Morton, D., Bond-Lamberty, B., Pereira, J. M. C., and Hurtt, G.: HESFIRE: a global fire model to explore the role of anthropogenic and weather drivers, Biogeosciences, 12, 887–903, doi:10.5194/bg-12-887-2015, 2015.

Leff, B., Ramankutty, N., and Foley, J.A.: Geographic distribution of major crops across the world, Glob. Biogeochem. Cycles, 18, GB1009, 2004.

Lenihan, J., Daly, C., Bachelet, D., and Neilson, R.: Simulating broad-scale fire severity in a dynamic global vegetation model, Northwest Sci., 72, 91–101, 1998.

Li, F., Levis, S., and Ward, D. S.: Quantifying the role of fire in the Earth system – Part 1: Improved global fire modeling in the Community Earth System Model (CESM1), Biogeosciences, 10, 2293–2314, doi:10.5194/bg-10-2293-2013, 2013.

Lin, H.-S., Jin, Y., Giglio, L., Foley, J.A., and Randerson, J.T.: Evaluating greenhouse gas emissions inventories for agricultural burning using satellite observations of active fires, Ecol. Apps., 22(4), 1345–1364, 2012.

Magi, B. I., Rabin, S., Shevliakova, E., and Pacala, S.: Separating agricultural and non-agricultural fire seasonality at regional scales, Biogeosciences, 9, 3003–3012, doi:10.5194/bg-9-3003-2012, 2012.

Marlon, J., Bartlein, P. J., Carcaillet, C., Gavin, D. G., Harrison, S. P., Higuera, P. E., Joos, F., Power, M. J., and Prentice, I. C.: Climate and human influences on global biomass burning over the past two millennia, Nat. Geosci., 1, 697–702, 2008.

Myhre, G., Shindell, D. T., Bréon, F.-M., Collins, W., Fuglestvedt, J., Huang, J., Koch, D., Lamarque, J.-F., Lee, D., Mendoza, B., Nakajima, T., Robock, A., Stephens, G., and Zhang, H.: Anthropogenic and Natural Radiative Forcing, Cambridge University Press, Cambridge, UK and New York, NY, USA, 659–740, 2013.

Olson, D. M., Dinerstein, E., Wikramanayake, E. D., Burgess, N. D., Powell, G. V., Underwood, E. C., D'amico, J. A., Itoua, I., Strand, H. E., and Morrison, J. C.: Terrestrial ecoregions of the world: a new map of life on Earth: a new global map of terrestrial ecoregions provides an innovative tool for conserving biodiversity, Bioscience, 51, 933–938, 2001.

Pechony, O. and Shindell, D. T.: Fire parameterization on a global scale, J. Geophys. Res., 114, D16115, doi:10.1029/2009JD011927, 2009.

Pfeiffer, M., Spessa, A., and Kaplan, J. O.: A model for global biomass burning in preindustrial time: LPJ-LMfire (v1.0), Geosci. Model Dev., 6, 643–685, doi:10.5194/gmd-6-643-2013, 2013.

~~Prentice, I. C., Kelley, D. I., Foster, P. N., Friedlingstein, P., Harrison, S. P., and Bartlein, P. J.: Modeling fire and the terrestrial carbon balance, Global Biogeochem. Cy., 25, GB3005, doi:10.1029/2010GB003906, 2011.~~

Pyne, S. J., Andrews, P. L., and Laven, R. D.: Fire and culture, in: Introduction to Wildland Fire, John Wiley and Sons, New York, 213–307, 1996a.

Pyne, S. J., Andrews, P. L., and Laven, R. D.: Fire ecology, in: Introduction to Wildland Fire, John Wiley and Sons, New York, 171–212, 1996b.

Randerson, J. T., Chen, Y., van der Werf, G. R., Rogers, B. M., and Morton, D. C.: Global burned area and biomass burning emissions from small fires, J. Geophys. Res., 117, G04012, doi:doi:10.1029/2012JG002128, 2012.

Scott, A. C., Bowman, D. M. J. S., Bond, W. J., Pyne, S., and Alexander, M. E.: Pyrogeography–temporal and spatial patterns of fire, in: Fire on Earth: An Introduction, John Wiley & Sons, West Sussex, UK, 113–129, 2014.

Seiler, W. and Crutzen, P. J.: Estimates of gross and net fluxes of carbon between the biosphere and the atmosphere from biomass burning, Climatic Change, 2, 207–247, 1980.

Taylor, K. E., Stouffer, R. J., and Meehl, G. A.: An overview of CMIP5 and the experiment design, B. Am. Meteorol. Soc., 93, 485–498, 2012.

Thonicke, K., Spessa, A., Prentice, I. C., Harrison, S. P., Dong, L., and Carmona-Moreno, C.: The influence of vegetation, fire spread and fire behaviour on biomass burning and trace gas emissions: results from a process-based model, Biogeosciences, 7, 1991–2011, doi:10.5194/bg-7-1991-2010, 2010.

Uhl, C. and Buschbacher, R.: A disturbing synergism between cattle ranch burning practices and selective tree harvesting in the eastern Amazon, Biotropica, 17, 265–268, 1985.

van Der Werf, G.R., Randerson, J.T., Giglio, L., Collatz, G.J., Mu, M., Kasibhatla, P.S., Morton, D.C., DeFries, R.S., Jin, Y., and van Leeuwen, T.T.: Global fire emissions and the contribution of deforestation, savanna, forest, agricultural, and peat fires (1997–2009), Atmos. Chem. Phys., 10, 11707–11735, 2010.

Venevsky, S., Thonicke, K., Sitch, S., and Cramer, W.: Simulating fire regimes in human-dominated ecosystems: Iberian Peninsula case study, Glob. Change Biol., 8, 984–998, 2002.

Ward, D. S., Kloster, S., Mahowald, N. M., Rogers, B. M., Randerson, J. T., and Hess, P. G.: The changing radiative forcing of fires: global model estimates for past, present and future, Atmos. Chem. Phys., 12, 10857–10886, doi:10.5194/acp-12-10857-2012, 2012.

Yevich, R. and Logan, J. A.: An assessment of biofuel use and burning of agricultural waste in the developing world, Global Biogeochem. Cy., 17, 1095, doi:10.1029/2002GB001952, 2003.

Table 1. List of GFED regions and abbreviations (Giglio et al., 2006).

Abbreviation	Full name
BONA	Boreal North America
TENA	Temperate North America
CEAM	Central America
NHSA	Northern Hemisphere South America
SHSA	Southern Hemisphere South America
EURO	Europe
MIDE	Middle East
NHAF	Northern Hemisphere Africa
SHAF	Southern Hemisphere Africa
BOAS	Boreal Asia
CEAS	Central Asia
SEAS	Southeast Asia
EQAS	Equatorial Asia
AUST	Australia and New Zealand

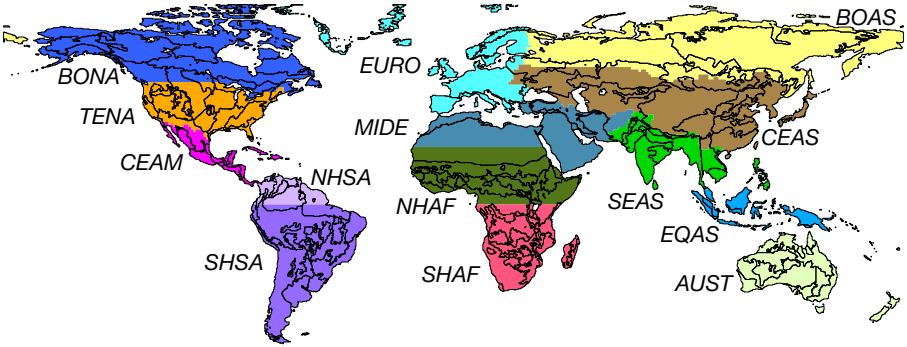

Figure 1. Regions used for analysis (outlines) overlaid on GFED regions (colors and labels; Giglio et al., 2006). See Table 1 for abbreviations. Shapefile with analysis regions available in Supplement.

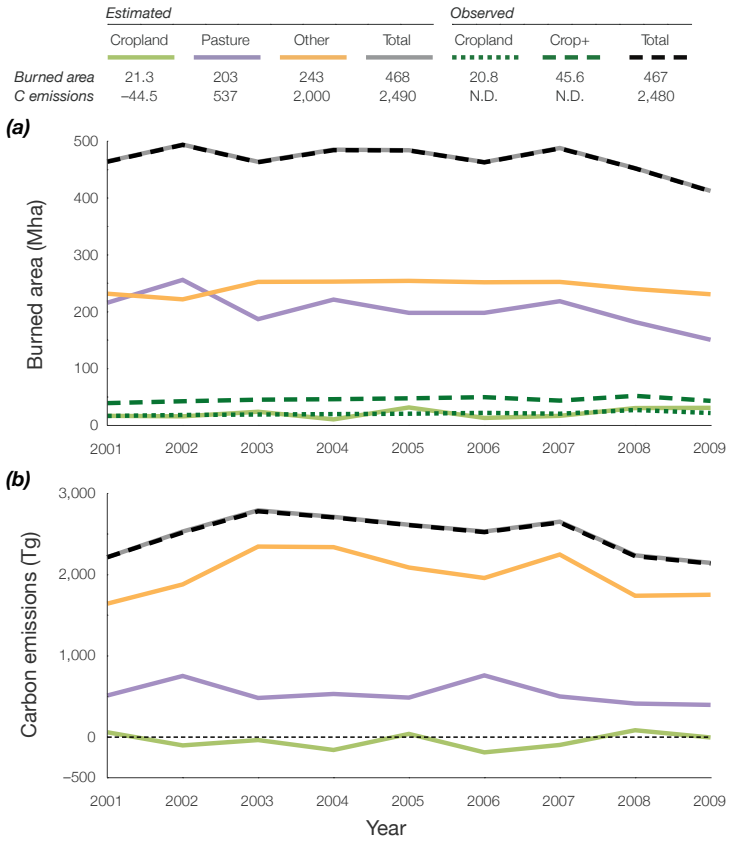

Figure 2. Observed and estimated annual timeseries of net observed and estimated global burned area (**a**~~,~~; Mha) and C emissions (**b**~~,~~; Tg = Mt). Numbers in table represent annual means. "N.D." = no data; "Crop+" = cropland + cropland-natural mosaic. Corresponds to Fig. ~~A1~~ S2 in ~~Appendix A~~ Supplemental Figures.

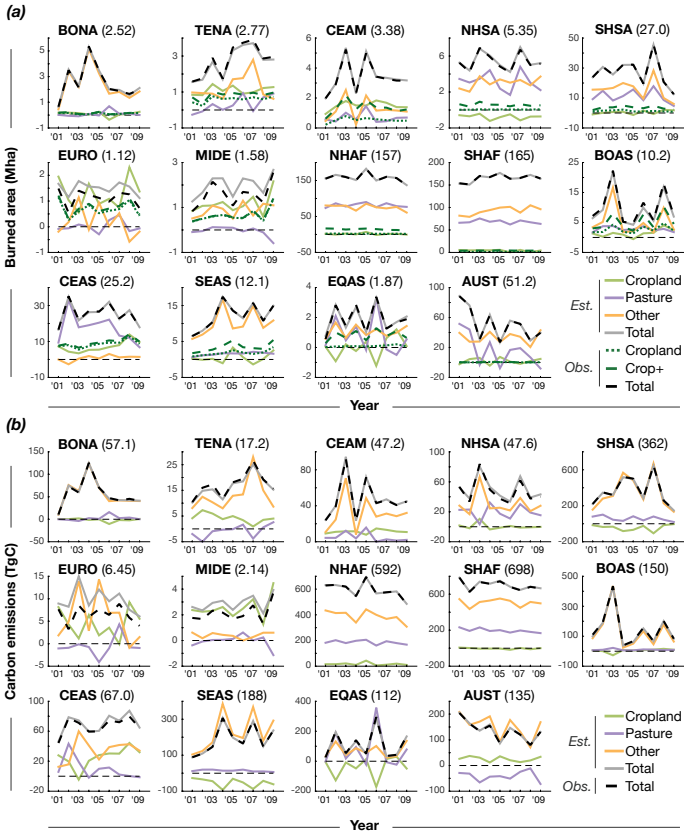

Figure 3. Annual timeseries of different fire types in each GFED region based on analysis of burned area (**a**; Mha) and C emissions (**b**; TgC). Numbers in parentheses next to region names represent mean annual observed fire there (either burned area or C emissions). "Crop+" refers to the combination of the land cover types "cropland" and "cropland-natural mosaic." Corresponds to Fig. ~~A2~~ S3 in ~~Appendix A~~ Supplemental Figures. Data available in Supplement.

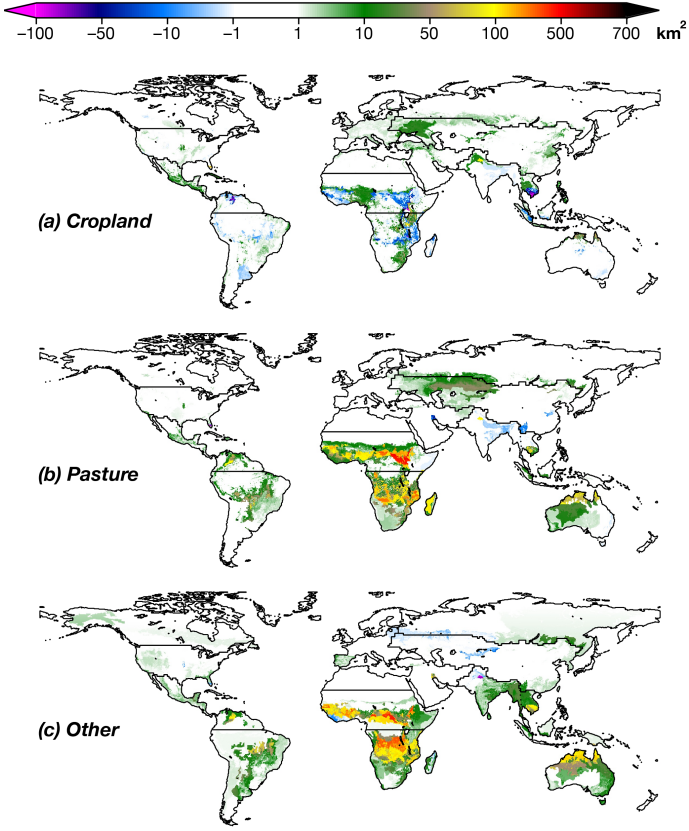

Figure 4. Maps of mean annual burned area (km^2) associated with **(a)** cropland, **(b)** pasture, and **(c)** other land. These are calculated from monthly maps generated by the equation $B_i = \widehat{F_k} A_{k,i}$ for each month and region. The r~~R~~esults can be interpreted as how much more (or less) fire would be expected if the area of the given land cover were to double (and the others remain the same). Corresponds to Fig. ~~A3~~ S5 in ~~Appendix A~~ Supplemental Figures. Compare with seasonal maps in Figs. S8–S11.

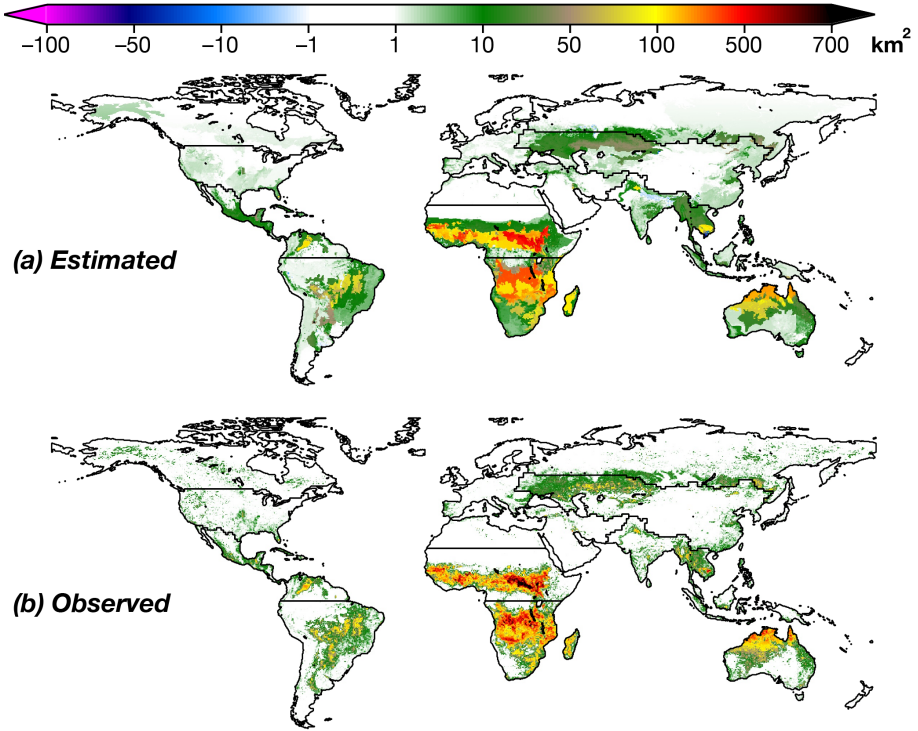

Figure 5. Maps of net mean annual total burned area (km^2): **(a)** Estimated. **(b)** Observed. Corresponds to Fig. ~~A4~~ S6 in ~~Appendix A~~ Supplemental Figures.

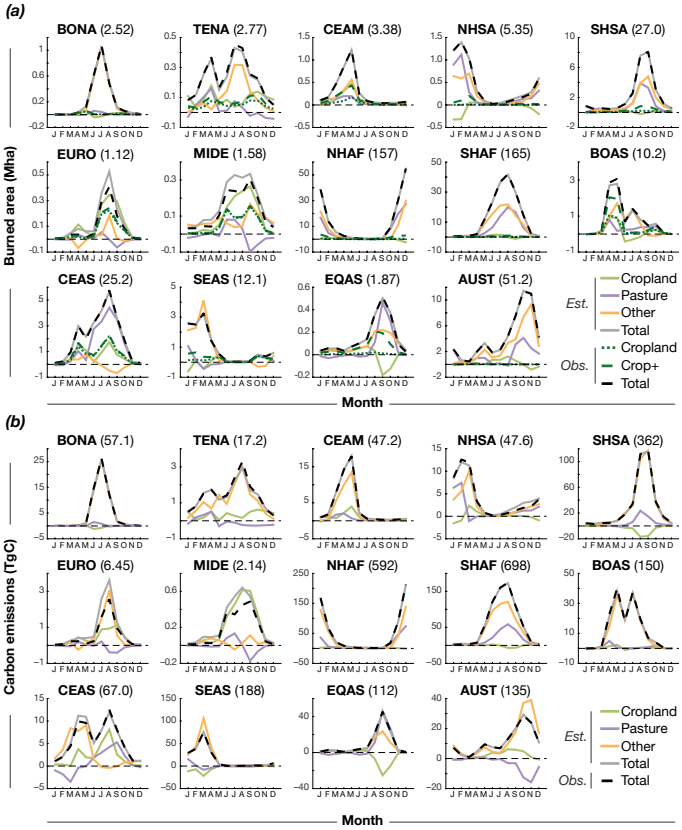

Figure 6. Seasonality of different fire types in each GFED region based on analysis of burned area (**a**; Mha) and C emissions (**b**; TgC). Numbers in parentheses next to region names represent mean annual observed fire there (either burned area or C emissions). Corresponds to Fig. ~~A5~~ S7 in ~~Appendix A~~ Supplemental Figures. Data available in Supplement.

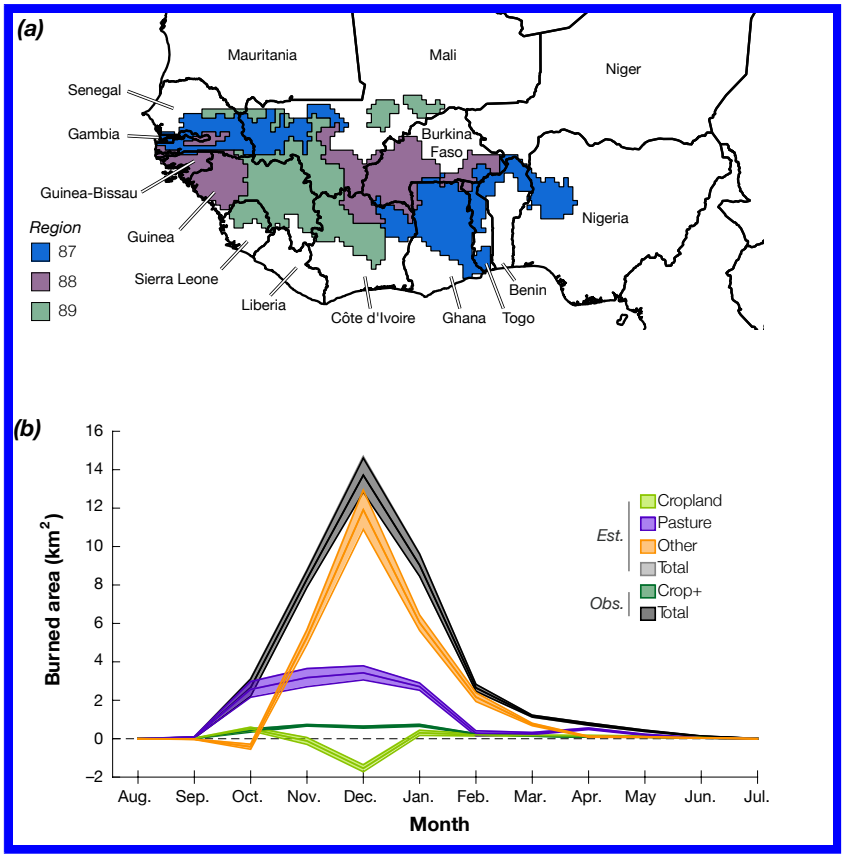
(a)
Mauritania
Mali
Niger
Senegal
Gambia
Burkina Faso
Guinea-Bissau
Guinea
Nigeria
Region
87
88
89
Sierra Leone
Liberia
Côte d'Ivoire
Ghana
Togo
Benin
(b)
Burned area (km²)
16
14
12
10
8
6
4
2
0
−2
Aug.
Sep.
Oct.
Nov.
Dec.
Jan.
Feb.
Mar.
Apr.
May
Jun.
Jul.
Month
Est.
Cropland
Pasture
Other
Total
Obs.
Crop+
Total

Figure 7. **(a)** Area included in West African case study, color-coded by analysis region. **(b)** Mean seasonality of burned area in ~~West African~~ case study regions. Shading represents interannual variability (± 1 SEM). Note that the X axis begins in August. Corresponds to Fig. ~~A6~~ S12 in ~~Appendix A~~ Supplemental Figures.

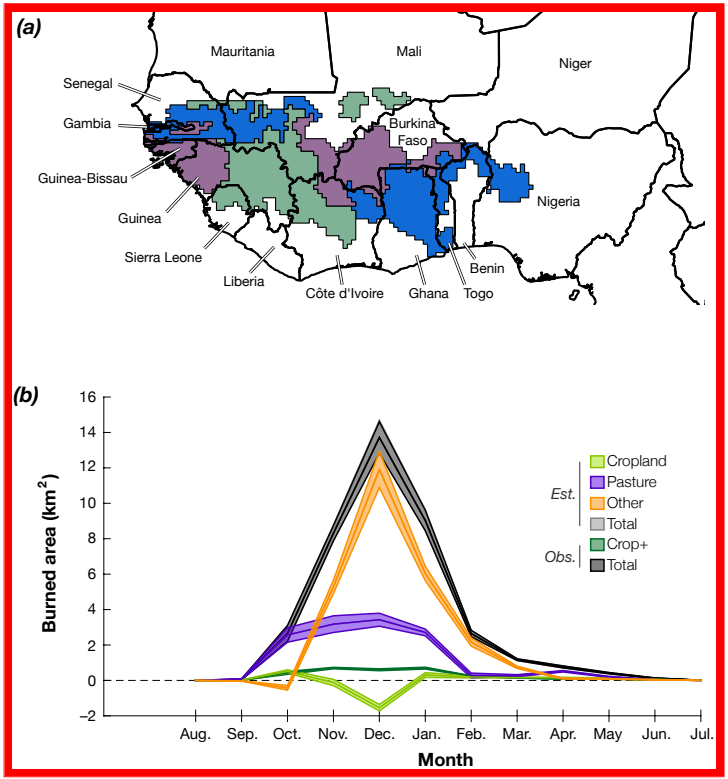

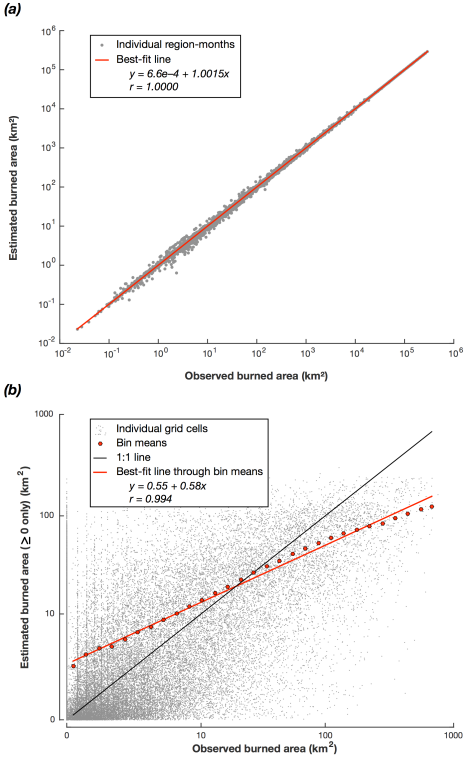
(a)
Individual region-months
Best-fit line
y = 6.6e–4 + 1.0015x
r = 1.0000
Estimated burned area (km²)
Observed burned area (km²)
(b)
Individual grid cells
Bin means
1:1 line
Best-fit line through bin means
y = 0.55 + 0.58x
r = 0.994
Estimated burned area (≥ 0 only) (km²)
Observed burned area (km²)

Figure 8. Scatter plots comparing estimated and observed total burned area ~~for **(a)** each analysis region and month (region-month), and **(b)** each grid cell. Values ≤ 0 not shown on scatter plots due to log-scale axes. Grid cells in region-months with no observed fire were excluded, as the analysis was not performed for such points. For **(b)**, regression performed on means of observed and estimated burned area for bins of observed burned area (red points), with minimum 100 grid cells required for a bin to be included. Also for **(b)**, $\frac{1}{75}$ of cells were chosen at random for scatter plotting.~~ . Gray points represent **(a)** each analysis region and month (region-month), or **(b)** individual grid cells ($\frac{1}{75}$ of cells chosen at random for plotting). Red lines represent the best-fit line from linear regression, with the regression in **(b)** fit to the red points, which represent mean observed and estimated values of grid cells in bins of observed burned area equally spaced along the X axis (with at least 100 grid cells required for a bin to be included). Values ≤ 0 not shown due to log-scale axes. Grid cells in region-months with no observed fire, where the analysis was not performed, were excluded from both plots and regressions. Corresponds to Fig. ~~A7~~ S13 in ~~Appendix A~~ Supplemental Figures.

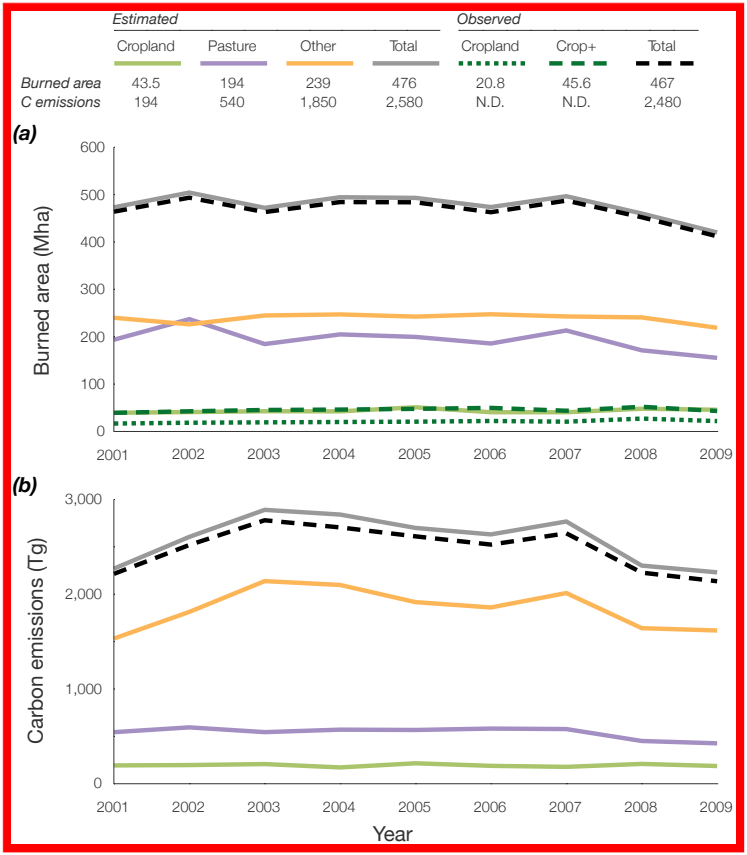

Figure A1. ~~Observed and estimated annual timeseries of net observed and estimated global burned area (**a**, Mha) and C emissions (**b**, Tg = Mt) from the constrained-$\widehat{F_k}$ analysis. Numbers in table represent annual means. "N.D." = no data; "Crop+" = cropland + cropland-natural mosaic. Corresponds to Fig. 2 in main text.~~

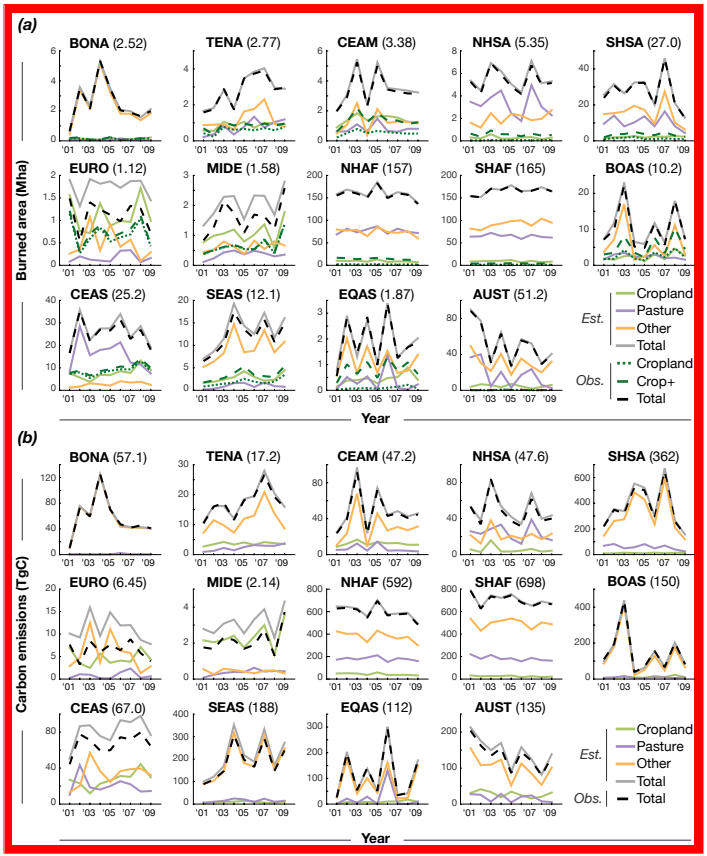

Figure A2. ~~Annual timeseries of different fire types in each GFED region based on constrained~~ $\widehat{F_k}$ ~~analysis of burned area (**a**; Mha) and C emissions (**b**; TgC). Numbers in parentheses next to region names represent mean annual observed fire there (either burned area or C emissions). Corresponds to Fig. 3 in main text.~~

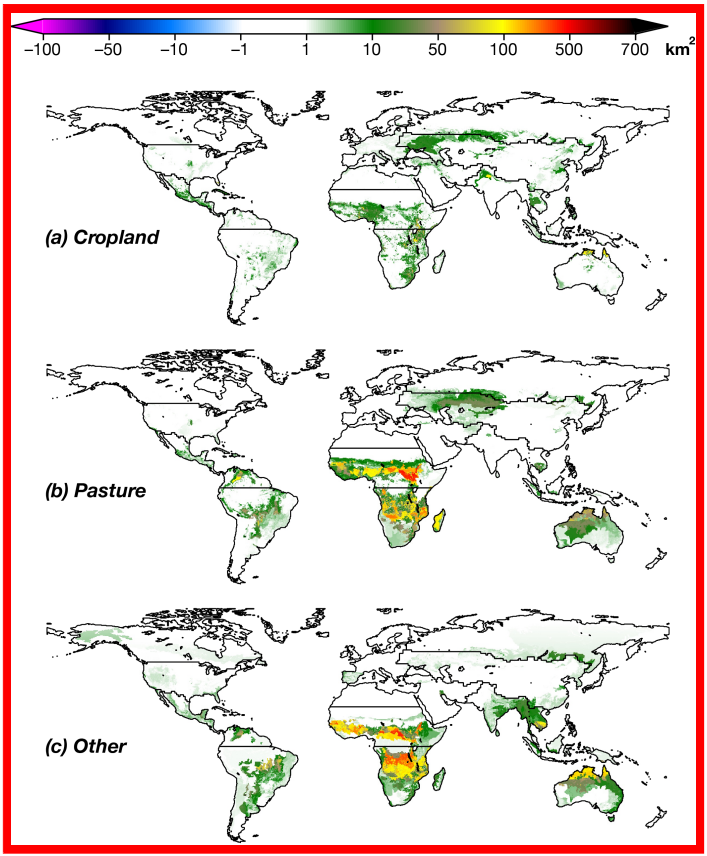

Figure A3. Maps, from constrained-$\widehat{F_k}$ analysis, of mean annual burned area (km^2) associated with **(a)** cropland, **(b)** pasture, and **(c)** other land. Numbers can be interpreted as how much more (or less) fire would be expected if the area of the given land cover were to double (and the others remain the same). Corresponds to Fig. 4 in main text.

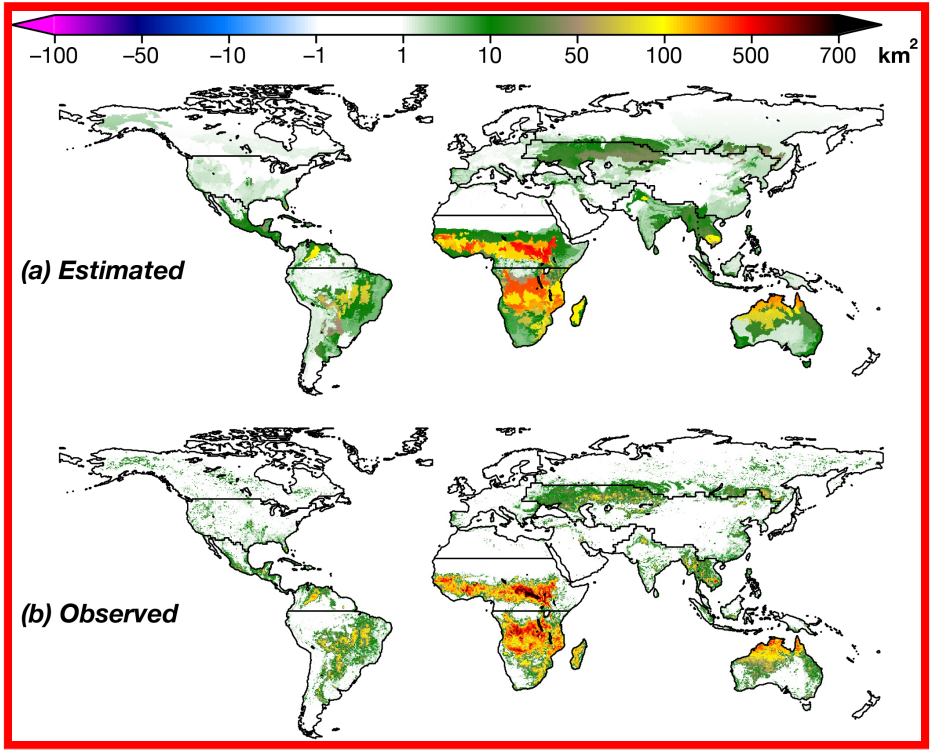

Figure A4. Maps of mean annual total burned area (km^2): **(a)** Estimated by constrained $\widehat{F_k}$ analysis. **(b)** Observed. Corresponds to Fig. 5 in main text.

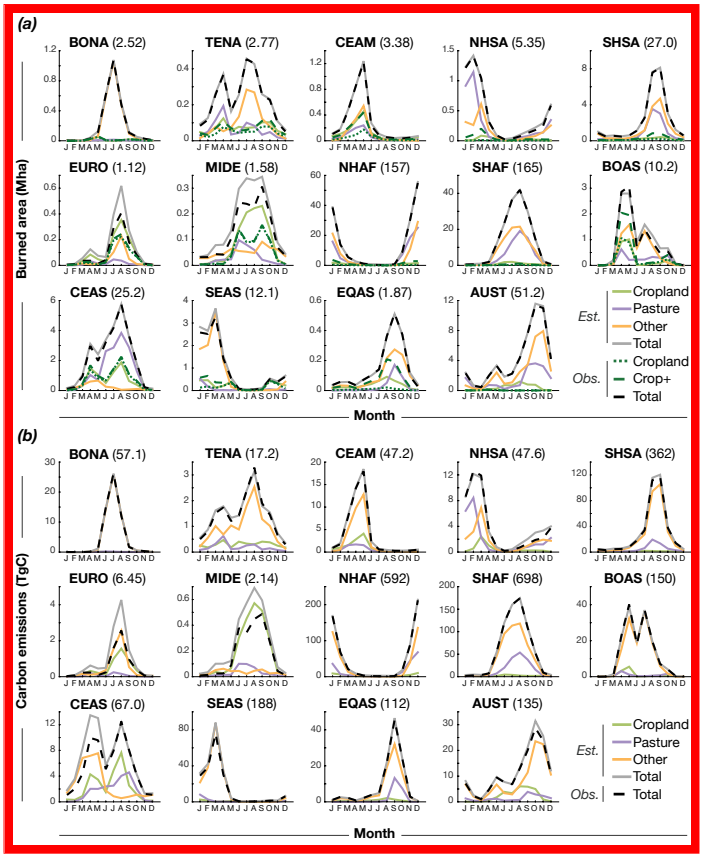

Figure A5. ~~Seasonality of different fire types in each GFED region based on constrained $\widehat{F_k}$ analysis of burned area (**a**; Mha) and C emissions (**b**; TgC). Numbers in parentheses next to region names represent mean annual observed fire there (either burned area or C emissions). Corresponds to Fig. 6 in main text.~~

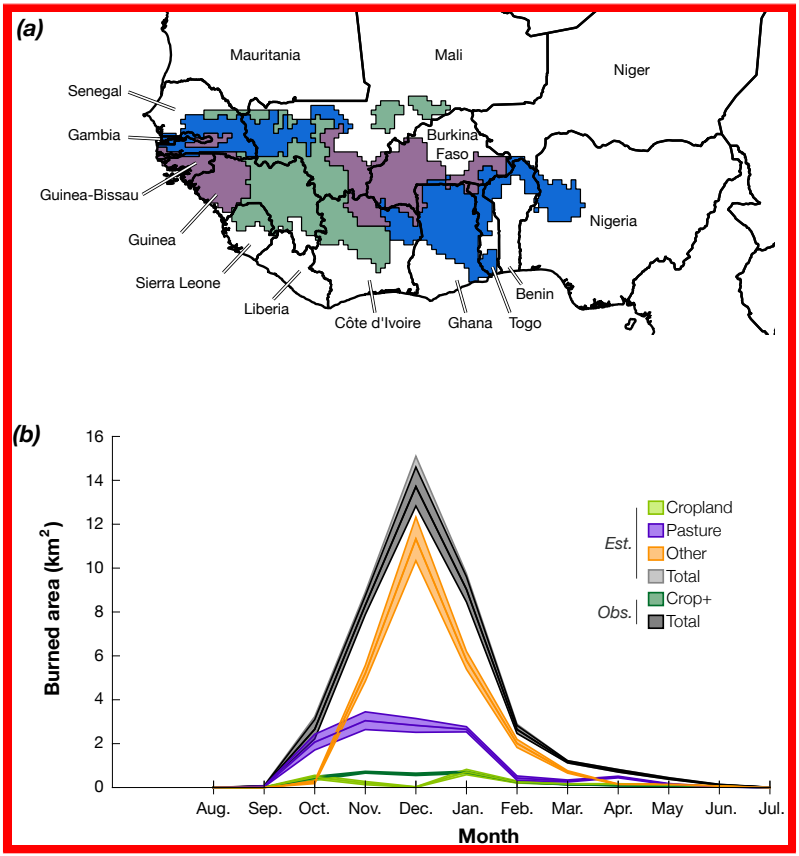

Figure A6. ~~Mean seasonality of burned area in West African case study regions based on constrained $\widehat{F_k}$ analysis. Shading represents interannual variability (± 1 SEM). Note that the X axis begins in August. Corresponds to Fig. 7 in main text.~~

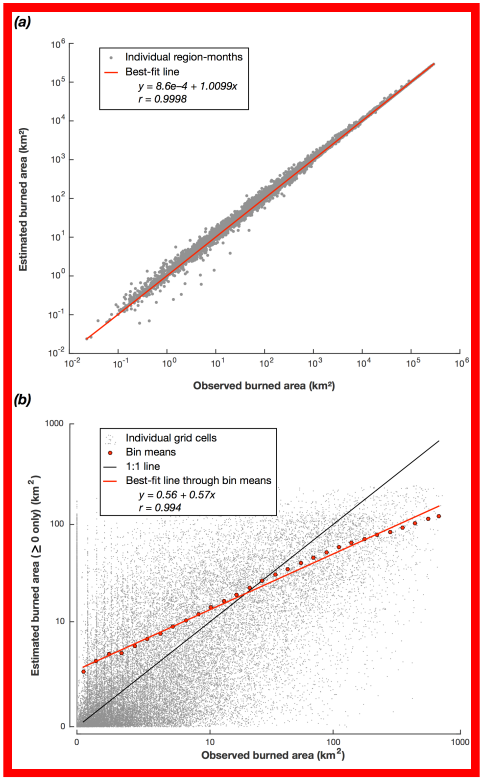

Figure A7. ~~Scatter plots comparing estimated burned area from constrained-$\widehat{F_k}$ analysis with observations for **(a)** each analysis region and month (region-month), and **(b)** each grid cell. Values ≤ 0 not shown on scatter plots due to log-scale axes. (Gridcells in) region-months with no observed fire were excluded, as the analysis was not performed for such points. For **(b)**, regression performed on means of observed and estimated burned area for bins of observed burned area (red points), with minimum 100 grid cells required for a bin to be included. Also for **(b)**, $\frac{1}{75}$ of cells were chosen at random for scatter plotting. Corresponds to Fig. 8 in main text.~~